PROCEEDINGS OF SCIENCE

The ATLAS ITk Strip Detector System for the Phase-II LHC Upgrade

Sven Wonsak*
On behalf of the ATLAS Collaboration
E-mail: s.wonsak@liverpoo.ac.uk

The ATLAS experiment at the Large Hadron Collider is currently preparing for a major upgrade of the Inner Tracking for the Phase-II LHC operation (known as HL-LHC), scheduled to start in 2026. In order to achieve the integrated luminosity of 4000 fb^{-1} over 10 years of operation, the instantaneous luminosity is expected to reach unprecedented values, resulting in about 200 proton-proton interactions in a typical bunch crossing. The radiation damage at the full integrated luminosity implies integrated hadron fluencies over $2\times10^{16}\,n_{eq}/cm^2$, requiring a complete replacement of the existing Inner Detector. An all-silicon Inner Tracker (ITk) is under development with a pixel detector surrounded by a strip detector, aiming to provide increased tracking coverage up to $|\eta| = 4$. The current prototyping, targeting an ITk Strip Detector system consisting of four barrel layers in the centre and forward regions composed of six disks at each end, is described in the ATLAS Inner Tracker Strip Detector Technical Design Report (TDR). With the recent final approval of the ITk strip TDR by the CERN Research Board, the prototyping phase is coming to an end and the pre-production readiness phase has started at the institutes involved. In this contribution an overview of the ITk strip detector components is given, including measurements of parts irradiated with a range of fluences reaching up to the predicted HL-LHC doses, demonstrating the excellent radiation hardness achieved.

ATL-ITK-PROC-2020-001
09/01/2020

The 28th International Workshop on Vertex Detectors - Vertex2019
13-18 October, 2019
Lopud, Croatia

*Speaker.

1. Introduction

In 2026 the upgraded High Luminosity Large Hadron Collider (HL-LHC) will start operating at an ultimate peak instantaneous luminosity of $7.5 \times 10^{34}\,\mathrm{cm}^{-2}\mathrm{s}^{-1}$, which corresponds to a mean of approximately 200 inelastic proton-proton collisions per beam crossing (pile-up) [2]. Over the more than ten years of operation the ATLAS detector aims for a total data set of $4000\,\mathrm{fb}^{-1}$. Because of this increased luminosity and the resulting expected radiation damage, the ATLAS Inner Detector [1] has to withstand an integrated hadron fluence of over $1.3\times10^{16}\,\mathrm{n_{eq}/cm^2}$ in the innermost pixel region and $1.6\times10^{15}\,\mathrm{n_{eq}/cm^2}$ in the strip system (see Figure 1). The current ATLAS Inner Detector (ID) would not be able to cope with the expected data rates and radiation damage. A new Inner Tracker (ITk), designed to operate in the HL-LHC and maintain low occupancy, will replace the current ATLAS ID.

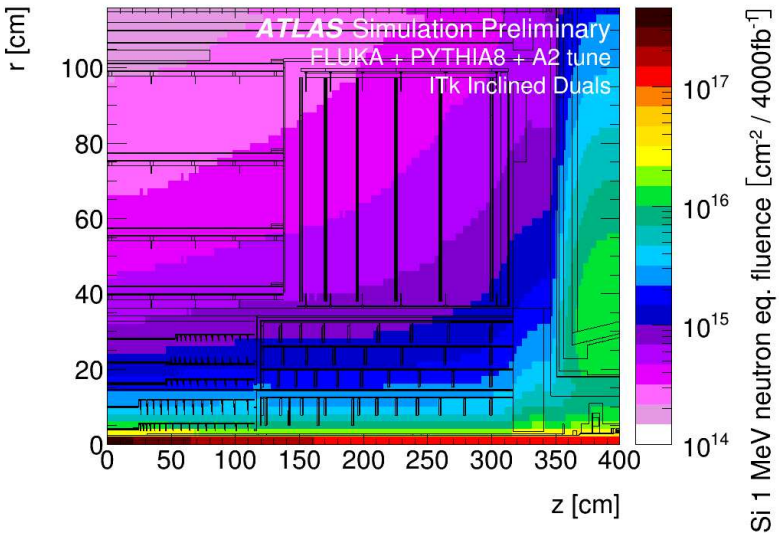

Figure 1: 1 MeV neutron equivalent fluence per $4000\,\mathrm{fb}^{-1}$ of integrated luminosity in the ATLAS Inner Tracker. Here only one quadrant and only active detector elements are shown. The horizontal axis is the axis along the beam pipe with zero being the interaction point [3].

The ITk will be an all-silicon tracking system that consists of a pixel detector at small radius close to the beam line and a large area strip tracker surrounding it. The pixel detector is built up of five central layers and an array of 30 rings with four different radii in the forward regions. For the strip region, four central (barrel) layers and six disks in each forward region (end-cap) will be built. The whole ITk will be approximately 6 m long, around 2 m in diameter, and covers up to a pseudo-rapidity of $|\eta| = 4$.

Figure 2 shows a schematic view of the ITk layout with the pixel layers indicated in red for the barrel layers and in dark red for the end-cap rings. The strip layers are indicated in blue for the barrel and dark blue for the end-cap. The final ITk strip system will comprise of approximately 18,000 modules with 60 million channels and cover an area of $165\,\mathrm{m}^2$ with silicon.

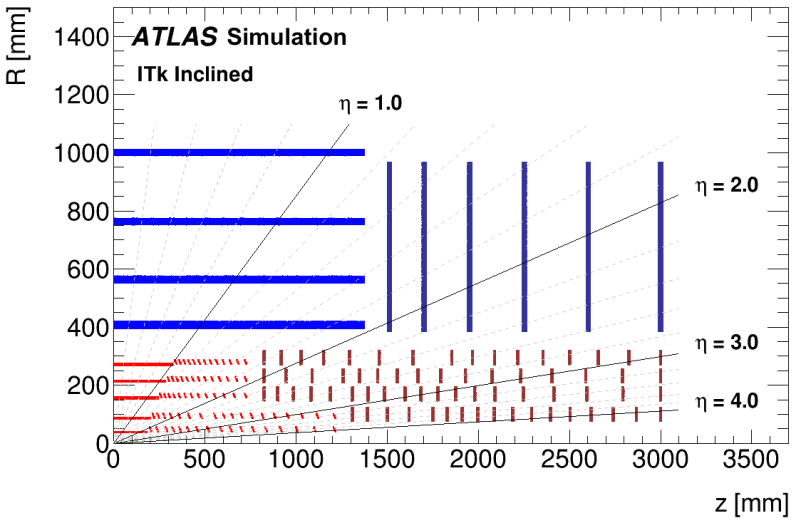

Figure 2: Schematic layout of the ITk for the HL-LHC phase of the ATLAS as presented in the Strip TDR [2]. The active elements of the strip barrel are shown in blue and end-cap Strip Detector in dark blue. For the Pixel Detector the sensors are shown in red for the barrel layers and in dark red for the end-cap rings. Here only one quadrant and only active detector elements are shown. The horizontal axis is the axis along the beam line with zero being the interaction point. The vertical axis is the radius measured from the interaction region.

2. The ITk Strip Detector

2.1 Local Support

Carbon fibre structures (cores) are used to support barrel and end-cap modules. The core is built from titanium cooling pipes embedded in thermally conductive foam and carbon fibre honeycomb. This design allows cooling down to -35°C utilizing evaporative CO_2. The core is enclosed in carbon fibre sheets (see Figure 3) and a polyimide bus tape is glued to the top and bottom of the stave, which contains the power and transmission lines for the silicon modules. An End-of-Substructure card (EoS) on each local support side is used for the electrical connection of the structure to other parts of the detector (power supplies, fibre-optic cables for data transfer).

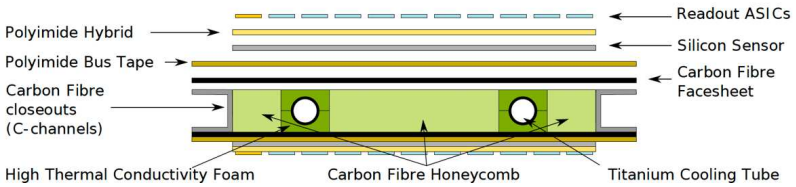

Figure 3: Schematic view of the local support structure [2].

Two different shapes of local support structures are used in the ITk. For the barrel region rectangular staves support 14 silicon modules on each side, the two innermost layers use short strip modules and the two outer layers long strip modules (see Figure 4). Within the whole barrel a total of 392 staves will be used. The end-caps use wedge-shaped petals with six modules on each side

(see Figure 5). Each disk consists of 32 petals and each end-cap houses six disks, which requires 384 petals to be built.

Figure 4: ITk barrel stave with 14 long strip modules. Each stave is 1.4 m long and 0.12 m wide.

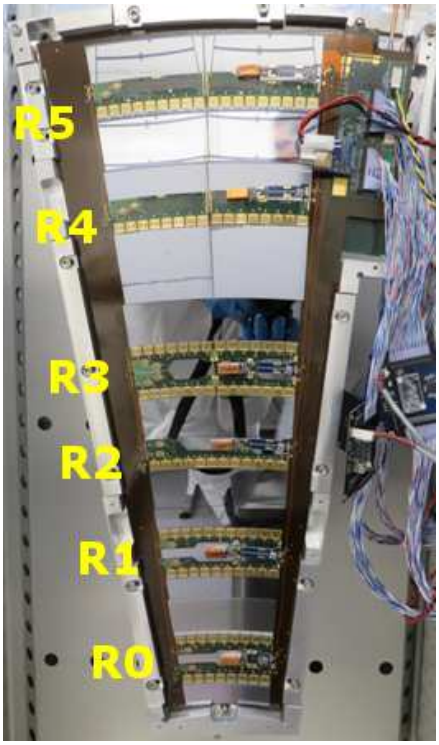

Figure 5: ITk end-cap petal, fully loaded with modules. The petal is 0.6 m high and at the top 0.3 m wide.

2.2 Modules

Modules are the basic building blocks of the strip detector and consist of one (or two) silicon sensors, up to four hybrids and up to one powerboard. Figure 6 shows a barrel short-strip module consisting of two hybrids, each with 10 ABCStar [4] and 1 HCCStar chips, one powerboard and a short-strip sensor. The hybrids are electronic circuit boards, made out of polyimide, and house the binary read-out chip ABCStar, each with 256 channels, and the hybrid controller chip (HCCStar). The hybrids utilize a star design topology, where the data from each front-end chip is directly routed to the HCCStar, where they are merged and transmitted at up to 640 Mbit/s to the EoS card. The hybrids receive their power from the powerboard (Figure 7). To minimize power losses, the bus-tape on the stave provides 10-11 V for all modules in parallel, in addition to the high voltage for the sensors, but the front-end chips only require 1.5 V. A DC-DC buck converter bPOL12V, developed at CERN [5], ensures a constant output voltage to power the hybrids. The autonomous monitor and control chip (AMAC), which is powered by a separate voltage converter LinPOL12V, is used for controlling the module and measuring among others temperature and high voltage current. Depending on the measurements, the AMAC can switch off a module, or prevent it from being switched on. On the local support structures, several modules share a common high voltage supply

line. The HVmux allows the switching of the high voltage of individual modules from a common bus on and off. Both, hybrids and powerboards are glued onto the silicon sensor with Polaris PF-7006 [6].

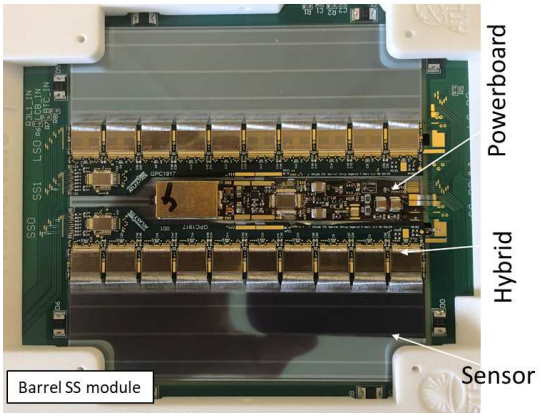

Figure 6: Picture of a barrel short strip module with two hybrids and one powerboard glued onto a sensor.

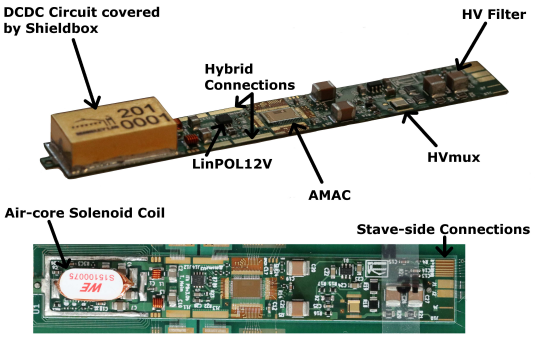

Figure 7: Barrel powerboard, containing high-voltage switch (HVmux), monitoring chip (AMAC) and DCDC power converter.

All sensors for the ITk strip detector will be produced by Hamamatsu Photonics [7] on 6-in wafers with p-type float zone bulk material and 320 μm thickness. Both barrel sensor types are $97.95 \times 97.62\,\text{mm}^2$ with a strip pitch of 75.5 μm. For the two inner barrel layers, the sensor is divided in four strip segments, each 24.12 mm long. The two outer layers have two segments with a strip length of 48.305 mm. To achieve the required Z resolution, the sensors are mounted at an angle of 26 mrad on the stave with respect to the beam line. In the end-caps six different sensor layouts are used with strip pitches from 69.9 μm to 80.7 μm and strip lengths from 15.1 mm to 60.2 mm. A stereo angle of 20 mrad is already built into the sensor design by having the strips not directly pointing to the interaction point [8]. The maximum bias voltage for all sensor types is 500 V.

2.3 Sensor Results

Full-sized sensors as well as mini-sensors have undergone an extensive test program to ensure the devices are fit for purpose and their behaviour at the expected end-of-life dose (2×10^{15} n_{eq}/cm^2 and 70 Mrad) is within specification. Charge collection measurements, performed at several institutes with mini-sensors irradiated with 24 GeV protons at the PS at CERN, with 70 MeV protons at CYRIC (Japan) and with thermal neutrons at Ljubljana have shown good agreement with the expected irradiation fluence dependence of the collected charge. Figure 8 shows a comparison of the charge collected from sensors irradiated with the different particle types and fluences at the maximum sensor bias voltage of 500 V. Comparing the production design sensors (A17) with similar sized prototype sensors (A12), produced by Hamamatsu Photonics, shows good agreement. As previously observed, the collected charge of sensors irradiated with neutrons is smaller than for sensors irradiated with protons to the same fluence [2]. Using the collected charge after neutron irradiation as benchmark, the sensors fulfil the requirement of a minimum signal-to-noise ratio of 10:1 at the end of life for all regions of the ITk strip detector.

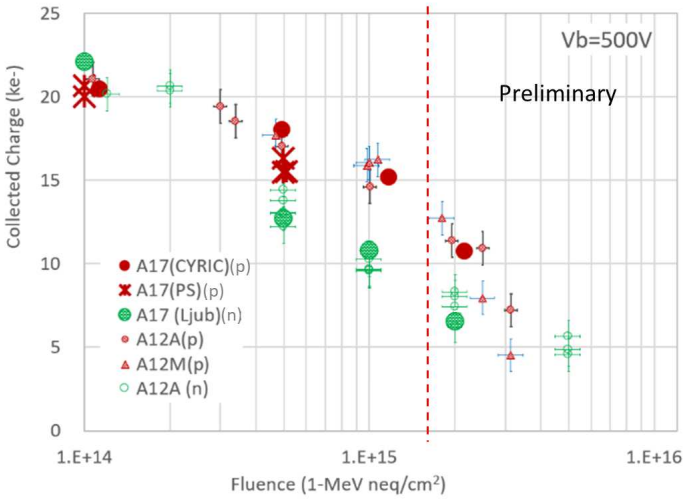

Figure 8: Collected charge of irradiated production sensors (A17) as function of irradiation fluence at 500 V, with the irradiation type colour coded. For comparison results from prototype sensors (A12) are shown as well. The maximum fluence expected at the end-of-lifetime is indicated by the dashed red line [9].

To investigate the effects of using thinner sensors, some production design sensors have been produced in the standard thickness of 320 μm, but with a thicker backside contact reducing the active thickness from approximately 300 μm to 240 μm. These "thin" sensors have been irradiated together with standard sensors to 5.1×10^{14} n_{eq}/cm^2 and 2×10^{15} n_{eq}/cm^2. The graphs in Figure 9 show that for unirradiated devices the collected charge of the "thin" sensor is clearly lower than for the standard device when the sensors are fully depleted and the collected charge becomes constant. For the irradiated sensors the measurements show that the collected charge is similar for both active thickness values, which indicates that in terms of collected charge there is no benefit for thinner sensors in the ITk operation range.

2.4 Hybrid Results

The hybrids are made out of polyimide cores with four copper layers to facilitate all the necessary routing for the star read-out configuration of the ASICs, using micro-vias for robust and reliable interconnection between the copper layers. The surface finish is ENIG to IPC specification 4552 to facilitate aluminium wedge wire-bonding. Several hybrids of the same type are produced on panels for maximum yield in the fabrication process. Because of the harsh environment the circuits have to be used in, test coupons have been designed for evaluation of the material and build. These are produced on the same panels as the hybrids and facilitate via-chains for micro-via reliability studies through thermal cycling, large bondable areas for wire-pull tests to determine the quality of the ENIG finish and capacitive plate structures to look for delamination during thermal cycling and irradiation.

Coupons are measured before and after passive component attachment, which includes an industrial reflow process at higher than 200°C. In Figure 10 the capacitance change is shown for 11 test coupons and it shows that the change is within the allowed tolerance of 10%. A decrease, that was not observed, would indicate delamination. Some test coupons have been irradiated with flu-

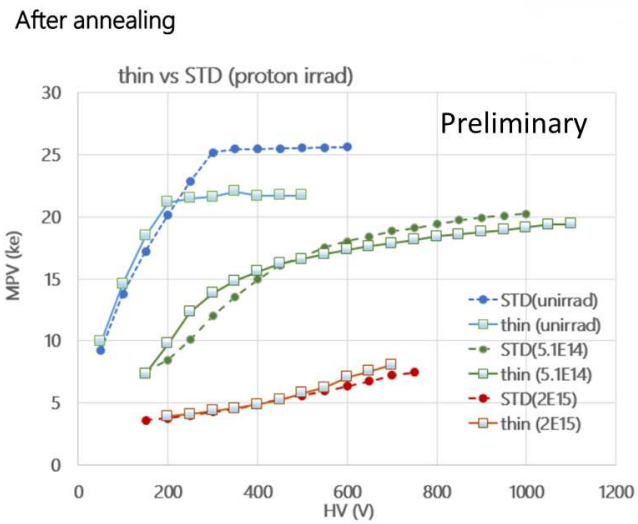

Figure 9: Comparison of irradiated sensors with standard active thickness (STD) of 300 μm and thin active thickness (thin) of 240 μm. Unirradiated sensors are shown in blue, sensors irradiated to 5.1×10^{14} n_{eq}/cm^2 in green and 2×10^{15} n_{eq}/cm^2 in red and annealed for 80 min at 60°C [9].

ences up to 1.1×10^{15} n_{eq}/cm^2. The capacitance measurements, shown in Figure 11 show changes below the accepted tolerance, indicating that the circuits can operate in the ITk detector.

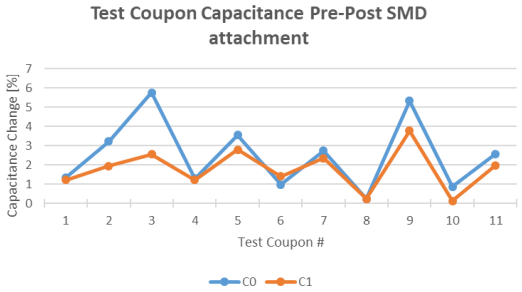

Figure 10: Capacitance change of test coupons after passive component attachment (reflow).

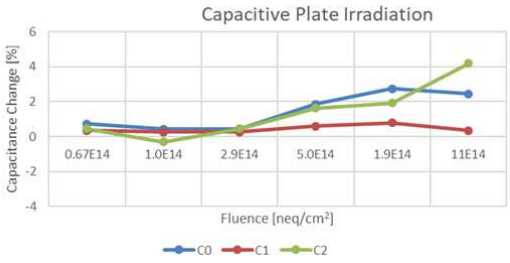

Figure 11: Capacitance change of irradiated test coupons up to 11×10^{14} n_{eq}/cm^2.

2.5 Powerboard Results

The autonomous monitor and control chip (AMAC) of the powerboard is powered by the LinPOL12V. Because the AMAC controls the ON/OFF state of the DCDC converter bPOL12V for the hybrids, it is important that the LinPOL12V is able to provide enough power at the current peak of the chip caused by the total ionizing dose (TID). AMACs have been irradiated with X-rays at a rate of 0.66 Mrad/hr up to 10 Mrad, whereas the TID peak was observed at approximately 1 Mrad (see Figure 12). The maximum current at the peak was approximately 70 mA for three different irradiation campaigns, which is within the specified range for the LinPOL12V.

One major heat source on the modules is the DCDC converter bPOL12V; with an efficiency of at least 70% it converts the 10-11 V from the bus tape to 1.5 V for the hybrids. It is important

to ensure the efficiency does not decrease below the 70% value at the expected end-of-lifetime irradiation, otherwise it would result in increased heating due to power loss. Figure 13 shows the efficiency as function of TID dose up to 90 Mrad dropping only approximately 1% and staying above 70%.

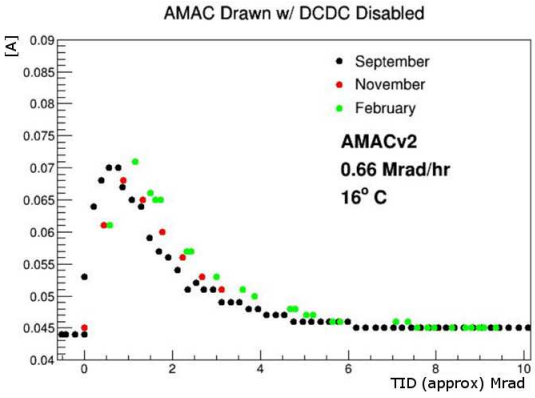

Figure 12: AMAC current as function of TID dose, measured at three different X-ray irradiation campaigns [10].

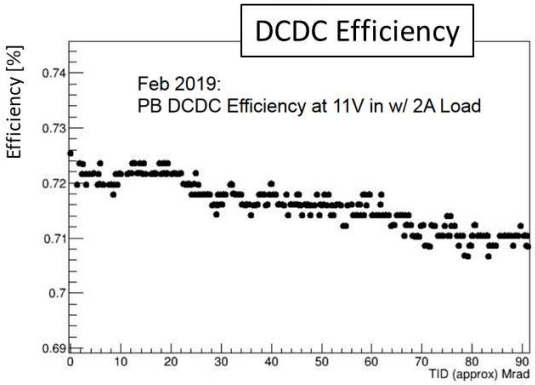

Figure 13: DCDC power converter efficiency as function of TID [10].

2.6 Module Results

To qualify modules for the use within the ITk a good understanding of the noise is important to fulfil the signal-to-noise requirement of at least 10:1. Single ABCStar chips as well as modules have been tested before and after irradiation. The measured noise as function of the input capacitance is shown in Figure 14. The single chip measurements show a good agreement before and after 80 Mrad irradiation and the results follow the expected trend, highlighted by the fitted lines. Measurements of ABCStar chips on prototype sensors (ATLAS12-EC, ATLAS17-LS and ATLAS12-SS) show in general higher noise values, but follow the same trend. The increased noise is expected and caused by the interstrip capacitance, which is currently not included in the graph. Measurements of an irradiated long-strip module are highlighted in blue circles. It shows two measurement points, which reflect the two strip segments where one is covered by the hybrid and therefore has increased capacitance. Both points match with the single chip measurements, not the other module measurements, because for the irradiated module the measurements were done at -20°C whereas all other measurements are at room temperature and the temperature dependency of the gain results in an approximately 10% change of the measured noise.

3. Conclusion

An extensive irradiation program for the silicon sensors and modules for the ATLAS ITk silicon strip tracker has shown that the new devices fulfil the requirements to reach a signal-to-noise ratio of at least 10:1 at the end-of-lifetime. Hybrids have shown to be within specification after having been irradiated and thermally stressed. Similarly, irradiation studies of the powerboard, which

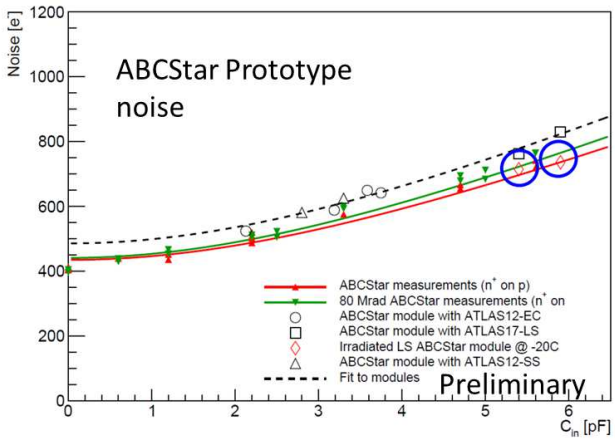

Figure 14: Noise comparison of single ABCStar chips and modules as function of input capacitance [10].

houses the AMAC and the DCDC converter bPOL12V, indicate the devices are fit for purpose within the harsh environment of the ITk.

After testing all components and finalising the design, all strip module assembly groups will start with the pre-production in 2020, in which 5% of the total number of ITk modules will be built to qualify the sites and training of production methods. The strip module production will start in 2021 and is expected to be finished towards the end of 2024, so that the strip barrel and endcap will be ready for integration in 2025.

References

[1] ATLAS Collaboration, *The ATLAS Experiment at the CERN Large Hadron Collider*, JINST 3 S08004 (2008).

[2] ATLAS Collaboration, *Technical Design Report for the ATLAS Inner Tracker Strip Detector*, CERN-LHCC-2017-005. ATLAS-TDR-025, https://cds.cern.ch/record/2257755.

[3] ATLAS Collaboration, *Phase II ITk Inclined Duals (April 2018)*, https://twiki.cern.ch/twiki/bin/view/AtlasPublic/RadiationSimulationPublicResults.

[4] W. Lu et al, *Development of the ABCStar front-end chip for the ATLAS silicon strip upgrade*, JINST 12 C04017 (2012).

[5] CERN, *Development of DCDC converters @ CERN*, https://project-dcdc.web.cern.ch/project-dcdc/.

[6] C. Helling, L. Poley, A.A. Affolder, V. Fadeyev, Z. Galloway, M. Gignac, S. Kachiguine, Z. Luce, Y. Unno, *Study of n-on-p sensors breakdown in presence of dielectrics placed on top surface*, Nucl. Instr. Meth. Phys. Res. A 924 (2019).

[7] *CERN Signs Three Contracts with Hamamatsu Potonics for ATLAS and CMS HL-LHC Upgrades*, https://procurement.web.cern.ch/node/1691.

[8] C. Lacasta et al., *Design of the first full size ATLAS ITk Strip sensor for the edcap region*, ATL-ITK-PROC-2018-010, https://cds.cern.ch/record/2305166.

[9] ATLAS ITk Strip Sensor Community, ATLAS ITk Strip Sensor FDR, April 2019.

[10] ATLAS ITk Strip Module Community, ATLAS ITk Strip Module FDR, September 2019.